NISTIR 4569

ANALYSIS OF OPTICAL FLOW ESTIMATION USING EPIPOLAR PLANE IMAGES

RAMESH RANGACHAR
Robotics Laboratory
Department of Mechanical Engineering
University of Maryland
College Park, Maryland 20742
Sensory Intelligence Group
and
Robot Systems Division

TSAI-HONG HONG
MARTIN HERMAN
Sensory Intelligence Group
Robot Systems Division

RANDALL LUCK
Aspex Incorporated
530 Broadway
New York, NY 10012

*U.S. DEPARTMENT OF COMMERCE
National Institute of Standards
and Technology
Manufacturing Engineering Laboratory
Gaithersburg, MD 20899

U.S. DEPARTMENT OF COMMERCE
Robert A. Mosbacher, Secretary
NATIONAL INSTITUTE OF STANDARDS
AND TECHNOLOGY
John W. Lyons, Director

NIST

NISTIR 4569

ANALYSIS OF OPTICAL FLOW ESTIMATION USING EPIPOLAR PLANE IMAGES

RAMESH RANGACHAR
Robotics Laboratory
Department of Mechanical Engineering
University of Maryland
College Park, Maryland 20742
Sensory Intelligence Group
and
Robot Systems Division

TSAI-HONG HONG
MARTIN HERMAN
Sensory Intelligence Group
Robot Systems Division

RANDALL LUCK
Aspex Incorporated
530 Broadway
New York, NY 10012

*U.S. DEPARTMENT OF COMMERCE
National Institute of Standards
and Technology
Manufacturing Engineering Laboratory
Gaithersburg, MD 20899

April 1991

U.S. DEPARTMENT OF COMMERCE
Robert A. Mosbacher, Secretary
NATIONAL INSTITUTE OF STANDARDS
AND TECHNOLOGY
John W. Lyons, Director

Analysis of Optical Flow Estimation Using Epipolar Plane Images

Ramesh Rangachar[1,3], Tsai-Hong Hong[1,2], Martin Herman[1], and Randall Luck[4]

[1]National Institute of Standards and Technology (NIST)
Bldg. 220, Rm B124, Gaithersburg, MD 20899

[2]Department of Computer Science and Information Systems
The American University, Washington, D.C. 20016

[3]Robotics Laboratory, Department of Mechanical Engineering
University of Maryland, College Park, MD 20742

[4]Aspex Incorporated, 530 Broadway, New York, NY 10012

ABSTRACT

Image flow, the apparent motion of brightness patterns on the image plane, can provide important visual information such as distance, shape, surface orientation, and boundaries. It can be determined by either feature tracking or spatio-temporal analysis. We consider spatio-temporal methods, and show how differential range can be estimated from time-space imagery.

We generate a time-space image by considering only one scan line of the image obtained from a camera moving in the horizontal direction at each time interval. At the next instant of time, we shift the previous line up by one pixel, and obtain another line from the image. We continue the procedure to obtain a time-space image, where each horizontal line represents the spatial relationship of the pixels, and each vertical line the temporal relationship.

Each feature along the horizontal scan line generates an edge in the time-space image, the slope of which depends upon the distance of the feature from the camera. We apply two mutually perpendicular edge operators to the time-space image, and determine the slope of each edge. We show that this corresponds to optical flow. We use the result to obtain the differential range, and show how this can be implemented on the Pipelined Image Processing Engine (PIPE).

We use a simple technique to calibrate the camera and show how the depth can be obtained from optical flow. We provide a statistical analysis of the results of 3-D reconstruction of the scenes using optical flow determined from 3×3, 5×5, and 7×7 edge operators.

1. INTRODUCTION

Image understanding is concerned with the determination of visual information such as distance, shape, surface orientation, boundaries, etc. One method of determining the visual information using monocular vision is to use optical flow, which is defined as the apparent motion of brightness patterns in the image plane. There are two methods to find the optical flow.

1. Feature matching based method. In this method, identifiable features from a sequence of images are extracted and correspondence is established. The corresponding features are used to calculate a set of disparity vectors for the sequence. Any identifiable entity can be used as a feature, but sharp, localized features give the best accuracy.

2. Spatio-temporal methods. These methods use the spatial and temporal relationships of image intensities to determine the optical flow. The time history of the position of a feature in the image can be represented in a 3-dimensional coordinate system (x,y,t). This is often called a spatio-temporal solid or spatio-temporal volume. The spatio-temporal area is defined as an $x-t$ slice of the solid, i.e., a slice taken with $y = constant$. The slope at any point (x,t) in the spatio-temporal area gives the horizontal component of its velocity. Therefore, the horizontal component of optical flow can be obtained by determining the orientation of the edges.

Our paper is organized as follows.

In section 2, we define optical flow, and show the equations for estimating optical flow using gradient based methods. We also show how to reconstruct a scene using optical flow. In section 3, we give a brief introduction to edge operators, and show how the magnitude and direction of edges can be extracted using edge operators. In section 4, we define an Epipolar Plane Image (EPI), and show how distance of objects from the camera is encoded in the EPI. Here, we use the results of sections 2 and 3 to show how optical flow, and hence the depth from the camera can be extracted from the spatio-temporal image. The algorithm and its implementation on PIPE are given in section 5. We describe our experimental setup and the experiments in section 6. In section 7, we provide several types of results such as *the differential range*, and *the number of misclassified points* in addition to the *mean* and *standard deviation* obtained from several types of edge operators.

2. MOTION FIELD AND OPTICAL FLOW

When the image of an object is formed on the image plane of the camera, every point P_o on the object results in a corresponding point P_i in the image. If P_o moves with a velocity v_o in the real world, then P_i moves with a velocity v_i in the image plane. Thus, all points on the object have a corresponding velocity vector in the image. These velocity vectors constitute the motion field. As the object moves, the brightness pattern in the image plane also moves. The apparent motion of the brightness pattern is known as optical flow. In an ideal situation, this corresponds to the motion field.[2]

Let us define two types of image motion: *local motion*, which is due to the motion of the objects in the environment, and *global motion*, which is due to the motion of the camera itself. By setting the *local motion* to zero, one can obtain an equation for the optical flow u induced by an object at a depth d in terms of the camera velocity V and its focal length f.

Using similar triangles OAB and OPQ, we get:

$$\frac{d}{f} = \frac{-V}{u}$$

$$u = \frac{-fV}{d}$$

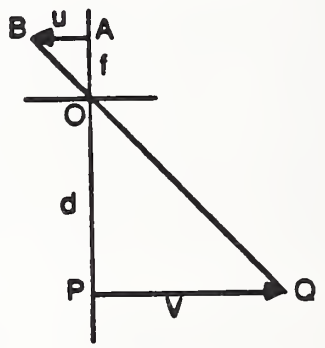

If the camera is moving with a uniform velocity V, then the numerator of the above equation is a constant. The equation can be written as follows.

$$u = \frac{-K}{d} \qquad (1)$$

The optical flow can be mathematically modelled and used as an estimate of the motion field, but this requires certain assumptions which are listed below.

1. The apparent velocity of brightness patterns is directly identified with the movement of the surfaces in the scene.
2. The surface being imaged is flat, and thus there is no variation in brightness due to shading effects.
3. Incidental illumination is uniform across the surface.

Under these assumptions, the brightness at a point in the image is proportional to the reflectance of the surface at the corresponding point on the object. As the reflectance varies smoothly and has no discontinuities, the image brightness is also continuous, and hence differentiable. This property of the image intensity is used by gradient based methods to determine the optical flow. In a gradient based method, the image intensity function $I(x,y,t)$ in the image plane at a point (x,y) and at time t is expanded using Taylor's series and used to compute the optical flow field.[5] The total derivative of the image intensity between two image frames separated by a very small time interval dt is zero.

$$\frac{dI(x,y,t)}{dt} = 0 \qquad (2)$$

It should be noted that this is strictly satisfied only for translation of a rigid body in planes parallel to the image plane. Using the chain rule of differentiation, equation (2) can be written as

$$\frac{dI}{dt} = \frac{\partial I}{\partial x}\frac{dx}{dt} + \frac{\partial I}{\partial y}\frac{dy}{dt} + \frac{\partial I}{\partial t} = 0 \qquad (3)$$

This can be written as

$$I_x u + I_y v + I_t = 0 \tag{4}$$

where u and v are the components of flow velocity in the x and y directions respectively, I_x and I_y are the spatial gradients, and I_t is the temporal gradient. I_x, I_y and I_t can be measured from the image sequence, and the optical flow (u, v) can be computed. Since we have two unknowns u and v, and one relationship in equation (4), the problem is considered ill-posed. In other words, we need one more constraint to regularize the problem and to compute the flow field. However, if the direction of motion of the camera is known, the optical flow can be computed using only one equation.

Consider a horizontally moving camera where the motion is considered to be along the x axis. Since the component of motion in the y direction is zero, equation (4) becomes

$$I_x u + I_t = 0$$

The optical flow in the x direction is given by

$$u = \frac{-I_t}{I_x} \tag{5}$$

The *magnitude* of optical flow is,

$$u = \frac{|-I_t|}{|I_x|} \tag{6}$$

The use of this method is justified in such situations where the direction of motion of the camera is known. Using Equations (1) and (5), an equation for the distance d of an object from the camera can be obtained.

$$d = \frac{KI_x}{I_t} \tag{7}$$

Thus, knowing K, one can reconstruct the 3D geometry of a scene. K can be determined either by determining f and V, or by using the EPI as shown section 4. In this work, we determine I_x and I_t using several edge operators on the EPI, and reconstruct the 3D geometry of the scene using Equation (7). We also provide a statistical analysis of the results from the different edge operators.

If there are two objects O_1 and O_2 at depths d_1 and d_2, respectively, from the camera, with $d_1 > d_2$, and they induce optical flow values u_1 and u_2, then we can derive the following from Equation (1):

$$\frac{d_1 - d_2}{d_1} = \frac{u_2 - u_1}{u_2} \tag{8}$$

We define Equation (8) as the differential range. The reasons why we calculate this function are

(i) Equation (8) is independent of V and f so that calibration of the camera is not required, and

(ii) we would like to determine the minimum distance between two objects that can be discriminated using optical flow, and express the result as a number which is independent of the depths of the objects from the camera.

3. EDGE DETECTION

An edge is a geometric form whose gray level is consistent on each of the two adjacent, extensive regions and changes abruptly as the border between the regions is crossed.[14] The pixel locations where this abrupt gray-level change occurs are called edge points. The derivative of a continuous image $I(x,y)$ has a local maximum in the direction perpendicular to the edge. The magnitude M and the direction Φ are given by the following equations.[6]

$$M = \left\{ \left[I_x \right]^2 + \left[I_y \right]^2 \right\}^{\frac{1}{2}} \tag{9}$$

$$\Phi = \tan^{-1} \left[\frac{I_y}{I_x} \right] \tag{10}$$

There are several different methods by which edges can be detected, and research is being continued to determine alternative methods. In this work, which is an application of edge operators to estimate optical flow, we have used gradient operators. The gradient operators have two mutually perpendicular masks H_x and H_y which are numerical approximations to I_x and I_y, respectively, and are used to determine M and Φ using equations (9) and (10). These operators give high signal to noise values at the edge points and zeroes for uniform regions. There are several gradient operators such as Prewitt, Sobel, isotropic, stochastic, etc. All of these can be easily implemented on digital hardware.

4. SPATIO-TEMPORAL IMAGE ANALYSIS

As discussed above, the time history of each feature point in the image gives the spatio-temporal volume, and a slice in the temporal direction gives the spatio-temporal area. Figure 1(a) shows a stationary scene containing a railroad car in the background and a tree in the foreground. Assume that the camera moves in the horizontal direction, that the optical axis of the camera points perpendicular to the direction of motion, and that the optical flow is in the negative direction. A horizontal scan line j of the image is selected and the spatio-temporal area for this scan line is obtained. When the scan line is coincident with the direction of motion of the camera, the spatio-temporal area is called the Epipolar Plane Image (EPI).[3] The EPI of the line j is shown in Figure 1(b). The slope due to the tree (closer object) is smaller than the slope due to the railroad car when the slope is measured from the time (vertical) axis. Thus, depending upon the distance of the objects along the scan line j, there will be lines of different slopes in the EPI. The greater the depth of the objects from the camera, the greater the slope measured from the time axis will be. If the slope can be measured, the distance between the camera and the object can be calculated.

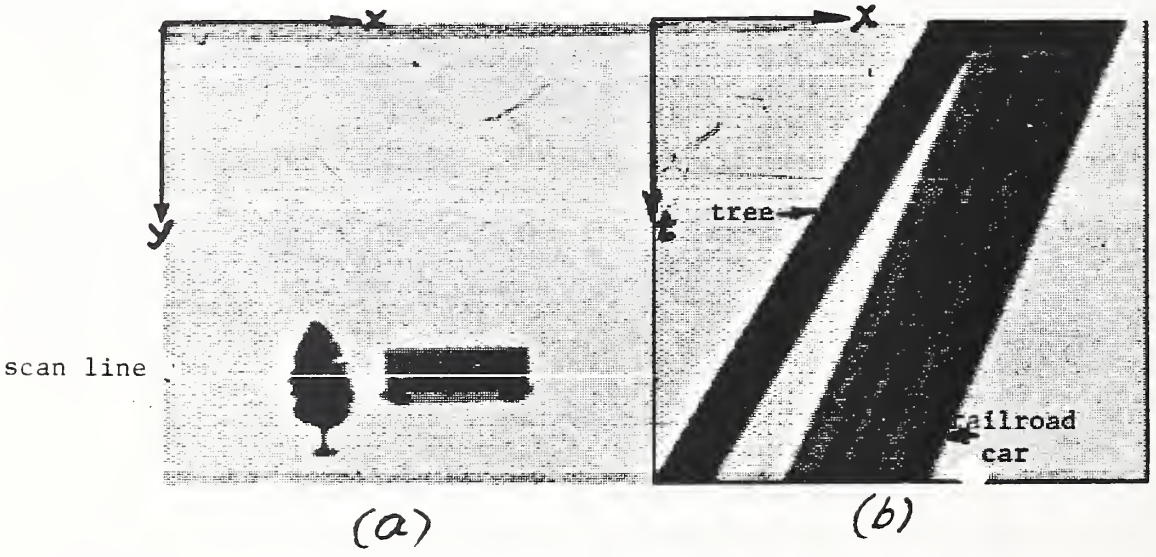

Figure 1: (a) Image at time k; (b) EPI for scan line j.

The use of time-space imagery for determining optical flow was first introduced by Bolles and Baker.[3] They determined slope by using a feature matching method. Here we take a different approach and use edge operators to determine the slope.

In section 2, we showed how optical flow can be obtained using the ratio of temporal difference over spatial difference (Equation 6). In an EPI, the horizontal axis represents space while the vertical axis represents time. Applying H_x to an EPI is similar to finding the spatial difference, while the application of H_y gives the temporal difference. If equation (10) is modified to determine the slope of a line in an EPI, and the variable y is changed to t, it can be written as follows:

$$\tan(\Phi) = \left[\frac{I_t}{I_x}\right] \tag{11}$$

Comparing equations (6) and (11), one can see that the two represent the same quantity. We use Equation (11) to determine optical flow in the EPI.

A closer look at Figure (1) and Equation (11) shows that the *global slope* of an object in the EPI is equal its optical flow. If we can obtain the EPI of an object at a known distance d from the camera and determine the *global* slope manually, we can determine the constant K using Equation (1). If the experiment is repeated with the same camera settings and the same value for V, and the spatial and temporal differences are determined using *local* edge operators, we can reconstruct the scene using Equation (7).

In section 3, it was stated that the gradient operators give high values at the edge points and zeroes for uniform regions. Therefore, optical flow will have high values at the edges and becomes indeterminate for uniform regions. The signal-to-noise of the flow is maximum at the edge and decreases as one moves away from it until it becomes indeterminate. To find a high signal-to-noise value for flow, the flow value at the edge must be extracted, while the flow values around the edge must be eliminated. We do this by determining the zero crossings of the Laplacian-Gaussian of the image and returning flow only at these zero crossing points.

We confine ourselves to small values of optical flow (less than 2 pixels per frame-time) because flow values significantly greater than zero are known to induce large measurement errors due to under-sampling.[7] We have implemented our algorithm to compute the optical flow on PIPE, which processes images at video rate.

5. PIPE IMPLEMENTATION

PIPE is a multi-stage, multi-pipelined image processing machine which may be used as the front-end of a real-time image understanding system. It was designed specifically for low level vision tasks at very high speed. It was conceived and designed at the National Institute of Standards and Technology (formerly National Bureau of Standards) by Kent, et al.[8] and is commercially available through Aspex Incorporated.[1] PIPE has a video stage to receive imagery, an input stage with four buffers, 1 to 8 identical Modular Processing Stages (MPSs) to process the imagery, and an output stage with four buffers to store images.

For further details on PIPE, refer to the references listed in this paper.[4,8-11,13,15]

In our experiments, we have used PIPE to obtain the optical flow to compute the differential range using 3×3, 5×5, and 7×7 edge operators. The algorithm to determine differential range of a selected scanline of an image has the following steps.

1. Obtain the EPI.
2. Determine the best estimate of optical flow.
3. Reconstruct the 3D geometry of the scene.

1. Obtain the EPI: We first create an EPI similar to Figure 1(*b*) in real time. Here we describe how the EPI for any selected scan line is obtained.

Figure 2 shows the steps to obtain the EPI for a selected scan line. The desired scan line is selected interactively using a program on the host computer. Figure 2(a) shows the image of an object and the selected scan line j at time t_1. Figure 2(b) shows only the scan line. This scan line is spread to the entire image as shown in Figure 2(c) using the image warping capability of PIPE. An image with a mask line at the bottom is ANDed with the spread image to shift the scan line to the bottom as shown in Figure 2(d). The steps explained above are repeated for another scan line at the next instant of time t_2. Figures 2(e) through (h) show the results at time t_2, where the image is shifted slightly to the left due to the horizontal motion of the camera. To obtain the EPI, the image at time t_1 (Figure 2d) is shifted up and added to the image at time t_2 (Figure 2h). Figure 2(k) shows the result at time t_2. The process is repeated for subsequent scan lines. Since we are using 256×242 images, it takes 242 cycles or 8 seconds to obtain the first EPI, but subsequent EPIs are formed in real-time by positioning the most recent line at the bottom of the EPI (Y=242) and shifting the previous scan lines up by one row.

2. Obtaining the best estimate of optical flow: This step begins with the previously obtained EPI. Figure 3 shows the data flow graph for this process. As indicated in the left branch of Figure 3, the EPI passes through two Neighborhood Operators (NOPs), where it is convolved with horizontal and vertical edge operators GRAD_X and GRAD_T respectively. The horizontal operator gives the spatial difference while the vertical operator gives the temporal difference. The outputs are then directed to a Two Valued Function (TVF) look up table called SLOPE which determines the

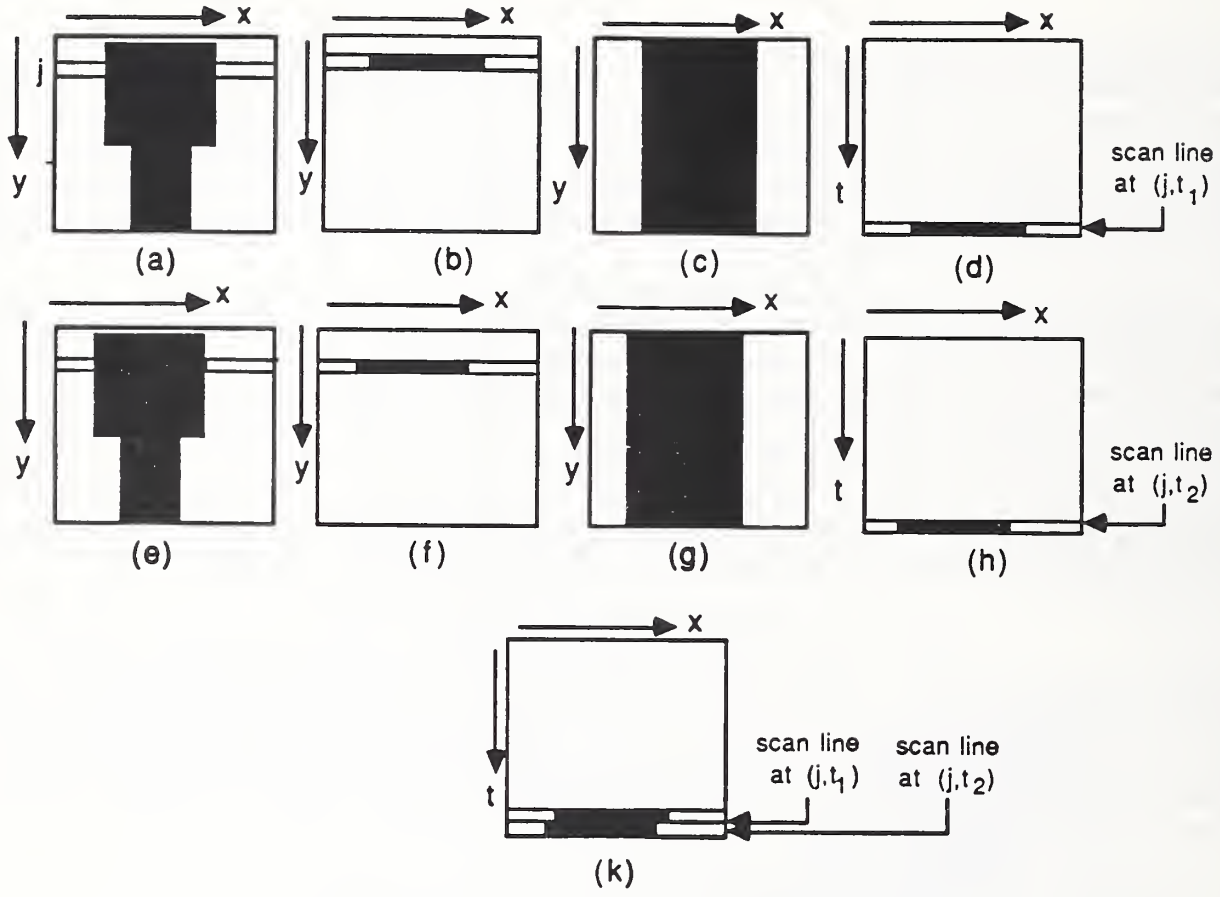

Figure 2: Steps to obtain the EPI. (a) Image of an object and the selected scan line at time t_1; (b) selected scan line at time t_1; (c) spread image of (b); (d) scan line at time t_1 shifted to bottom of EPI; (e), (f), (g) and (h) similar results at time t_2; (k) image (d) shifted up and added to (h).

slope, and hence the optical flow using Equation (11).

As mentioned earlier, in order to obtain the best estimate of optical flow, the zero crossings of the Laplacian-Gaussian of the image are used as a mask to determine where optical flow is returned. The right branch in Figure 3 shows how the zero crossings are determined. The EPI is passed through the difference of two Gaussians (which is equivalent to a Laplacian-Gaussian operator). The output is passed through a boolean neighborhood operator where the zero crossings are determined. The zero crossings are then ANDed with the optical flow image from the TVF to obtain the best estimate of the optical flow.

3. Segmentation of optical flow: It has been shown (Equation (1)) that optical flow is inversely proportional to the depth. Therefore, segmenting the optical flow is equivalent to segmenting depth. This is performed by using an interactive program from the host computer.

FOR each pixel

IF (*flow* < *threshold*) *THEN intensity* = 0

ELSE intensity = 255

Consider two objects O_1 and O_2 at depths d_1 and d_2 from the camera, respectively, with $(d_1 > d_2)$. These give rise to optical flow values u_1 and u_2 $(u_1 < u_2)$, respectively. We interactively vary the threshold in the program shown above until the flow due to the object at depth d_1 disappears from the scene while the flow due to the object at distance d_2 remains. We thus say that we have discriminated between objects O_1 and O_2. By physically measuring the values d_1 and d_2, we can calculate the *range discriminability* r_d using the following equation obtained from Equation (1).

$$r_d(\%) = \frac{(d_1 - d_2)}{d_1} \times 100 \tag{12}$$

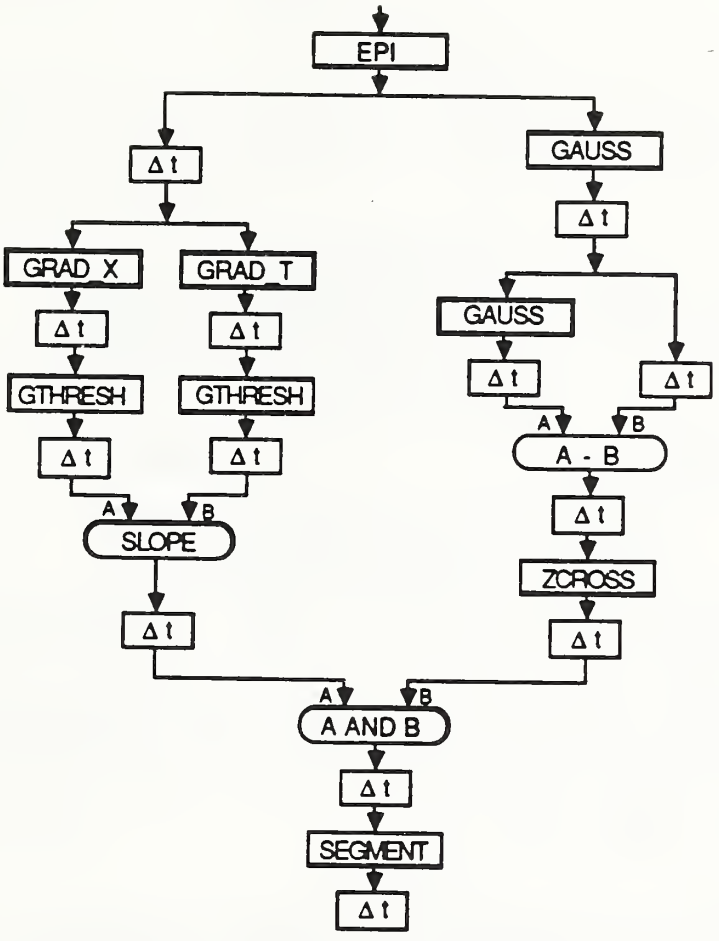

Figure 3: Data flow graph to determine the slope.

To compute the statistics, we have developed computer programs on the Sun computer. We obtain the EPI and the zero crossings using the PIPE. We use the Sun for 3-D reconstruction of the scene and subsequent statistical analysis.

6. EXPERIMENTS, RESULTS AND DISCUSSION

A top view of the setup for our experiments is shown in Figure 4. We use an optical rail which has two platforms as shown in the figure: one translates horizontally and the other rotates about a vertical axis. The camera is mounted on the platforms as shown. The accuracy of the velocity of translation is within 0.02% of the selected velocity.

We experimented with 3×3, 5×5, and 7×7 edge operators. Since PIPE performs only 3×3 neighborhood operations, we first used 3×3 edge operators. The experiment was repeated using 5×5 and 7×7 edge operators. 5×5 and 7×7 edge operators are approximated by products of 3×3 convolutions.[12]

Objects (O_1, O_2) were placed at different depths from the camera (d_1, d_2) and the optical flow was determined. Segmentation was performed on the optical flow and the range differential was calculated. The experiment was repeated by decreasing the difference d_1–d_2 until further segmentation was not possible. The optical flow was thresholded to determine the discriminability of the method. The range discriminability calculated using Equation (12) was 18%.

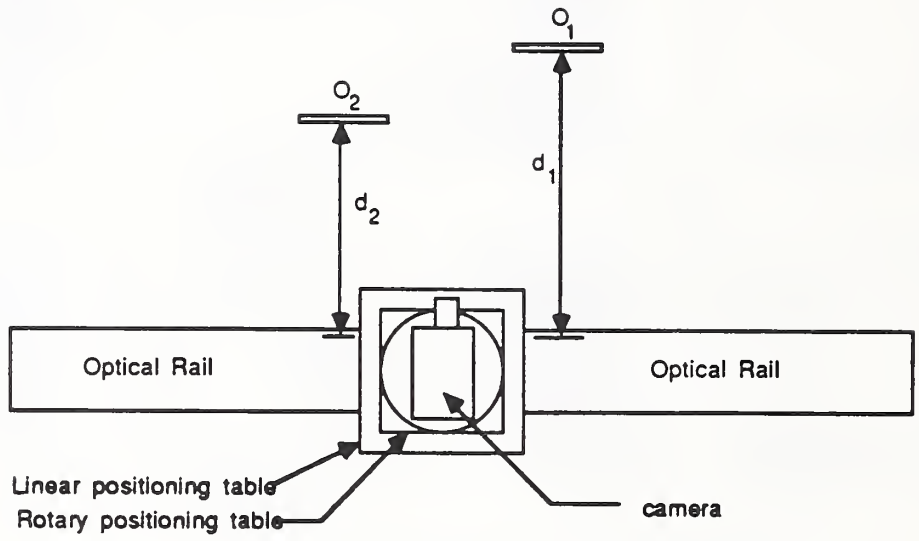

Figure 4: Experimental setup.

To compare the different methods, we determine *the number of misclassified points* (N_{miss}) for each method. N_{miss} is determined as follows.

The two objects O_1 and O_2 are placed as shown in Figure 4. The threshold for making the optical flow due to object O_1 disappear is determined. Knowing this value (*threshold*), a three-level segmentation is performed as follows.

FOR each pixel

IF $(flow < noise\text{-}level)$ *THEN intensity* $= 0$

IF $(flow < threshold)$ *THEN intensity* $= 128$

ELSE intensity $= 255$

This program segments an image such that the image will have an intensity value of 128 for the object in the background and 255 for the one in the foreground. However, at points where there is no optical flow, the image intensity is zero. To determine N_{miss}, a 5×5 window of the image is considered. Since the two objects in the scene are far apart, the image intensity in the small window is expected to be either 255 or 128 and zero. The total number of non-zero points are considered "classified points". However, if the intensity values in the selected window are 255, 128, and zero, then the points with intensity value 255 and those with intensity value 128 are summed separately. The one having a lower value for the sum is considered "misclassified". The procedure is repeated for the entire image and the total number of misclassified points as well as the total number of non-zero points is determined. N_{miss} is calculated using the following equation.

$$N_{miss} = \frac{total\ number\ of\ misclassified\ points}{total\ number\ of\ points\ in\ the\ image}$$

N_{miss} was 7.1% when the 3×3 operator was used. When the 5×5 operator was used, N_{miss} reduced significantly to 3.6%. When the 7×7 operator was used, N_{miss} was 2.9%. The reduction in N_{miss} was not significant in the latter case, because the approximate convolution had a small error. However, the experiment proved that the results can be improved by using convolutions of higher order.

The following experiments to be described involved using optical flow to determine the depth from the camera. First, K was determined as follows. If an object is placed at a known depth d from the camera and the resulting optical flow u is determined, then K can be determined from Equation (1). Since it is difficult to physically measure the exact depth d of a single object from the *focal point* of the camera, we used two objects at depths d_1 and d_2 from the camera. The difference in the depths d_1–d_2 was accurately measured using a ruler. The optical flow values u_1 and u_2 due

to the two objects were determined by manually measuring their corresponding slopes in the resultant EPI. K was determined using the following equation.

$$K = \frac{(d_2 - d_1)u_1u_2}{(u_1+u_2)}$$

The subsequent experiments were repeated with the *same* camera settings and the *same* velocity, and hence the *same* K. We used two objects O_1 and O_2 at depths d_1 and d_2 and determined the depth from the camera using 3×3, 5×5, and 7×7 operators. We also computed the mean and the standard deviations of the results obtained from our experiments. The results are summarized below.

Results Using Edge Operators (Farther Object)		
Size	Mean (mm)	Standard Deviation (mm)
3×3	1022	463
5×5	1239	104
7×7	1337	64

Results Using Edge Operators (Nearer Object)		
Size	Mean (mm)	Standard Deviation (mm)
3×3	909	589
5×5	975	102
7×7	1065	45

Our results show that better results can be obtained by increasing the size of the edge operators. The results from 3×3 operators have a large error in the mean, and a wide deviation from the mean. The results can be improved by using 5×5 and 7×7 edge operators.

7. CONCLUSION

Depth from motion can be obtained in a variety of ways, using different techniques. EPI analysis can be used to determine optical flow using edge operators. The algorithm has been implemented on PIPE and results have been obtained in real time. The accuracy of the method is dependent on the size of the edge operator used, but real time implementation on PIPE becomes difficult as the size of the operator increases. The optical flow determined will have high values near the edge and becomes indeterminate for uniform regions, with the best estimate being at the center of the edge. Zero crossings of the Laplacian-Gaussian of the image have been used to localize these edge points. Statistical analysis of the results of the edge operators confirms the fact that better vaues for the mean and the standard deviation of the depth can be obtained by increasing the size of the edge operators.

ACKNOWLEDGEMENTS

This work has been supported by the U.S. Army Laboratory Command, Human Engineering Laboratory and Harry Diamond Laboratories, and by the Defense Advanced Research Projects Agency (DARPA), Tactical Technology Office. Special thanks go to Mr. Charles M. Shoemaker, formerly of the Human Engineering Laboratory, to Dr. Philip Emmerman of Harry Diamond Laboratories, and to Dr. Jasper Lupo of DARPA for their direction and guidance. We also thank Don Orser and Marilyn Nashman of NIST for their valuable comments and suggestions.

REFERENCES

1. *The PIPE User's Manual*, Aspex, 1987. 530 Broadway, New York, NY 10012
2. Horn, B.K.P., et al., *Robot Vision*, MIT Press, Cambridge, Mass., 1986.

3. Bolles, R.C., Baker, H.H., and Marimont, D.H., "Epipolar-Plane Image Analysis: An Approach to Determining Structure from Motion," *International Journal of Computer Vision 1:7-55*, 1987.

4. Herman, M., "Application of the PIPE Image Processing Machine to Scanning Microscopy," *Proc. SPIE Scanning Microscopy Technologies and Applications*, vol. 897, pp. 169-173, Los Angeles, CA., January 1988.

5. Horn, B.K.P. and Schunk, B.G., "Determining Optical Flow," *Artificial Intelligence*, vol. 17, pp. 185-203, 1981.

6. Jain, A. K., *Fundamentals of Digital Image Processing*, Prentice-Hall, Inc., Englewood Cliffs, New Jersy, 1989.

7. Kearney, J.K., Thompson, W.B., and Boley, D.L., "Optical Flow Estimation: An Error Analysis of Gradient-Based Methods with Local Optimization," *IEEE Transactions on Pattern Analysis and Machine Intelligence*, vol. PAMI-9, no. 2, pp. 229-244, March 1987.

8. Kent, E.W., Shneier, M.O., and Lumia, R., "PIPE (Pipelined Image Processing Engine)," *J. Parallel and Distributed Computing*, pp. 50-78, 1985.

9. Luck, R.L., "PIPE: a Parallel Processor for Dynamic Image Processing," in *Image Understanding and Man-Machine Interface*, ed. Pearson, J.J. Barett, E., pp. 109-115 , Proc. SPIE 758, 1987.

10. Luck, R.L., "An overview of the PIPE Systems," *Proc. Third Intl. Conference on Super Computing*, vol. 3, pp. 69-78, Boston, 1988.

11. Nashman, M. and Chaconas, K., *Low Level Image Processing Techniques Using the Pipelined Image Processing Engine in the Flight Telerobotic Servicer*, Robot Systems Division, National Institute of Standards and Technology, 1989.

12. O'Leary, D.P., "Some Algorithms for Approximating Convolutions," *Computer Vision, Graphics, and Image Processing*, no. 41, pp. 333-345, 1988.

13. Rangachar, R., Hong, T.-H., Herman, M., and Lupo, J., "Real-Time Implementation of a Differential Range Finder," *Proc. SPIE Real-Time Image Processing II: Algorithms, Architectures, and Applications*, Orlando, Florida, April 1990.

14. Rosenfeld, A. and Kak, A.C., *Digital Picture Processing, Vol 2.*, Academic Press, Inc., Orlando, Florida , 1982.

15. Singh, A., "Image Processing on PIPE," Technical Report TN-87-093, Philips Laboratories, Briarcliff Manor, New York, 1987.

NIST-114A
(REV. 3-90)

U.S. DEPARTMENT OF COMMERCE
NATIONAL INSTITUTE OF STANDARDS AND TECHNOLOGY

BIBLIOGRAPHIC DATA SHEET

1. PUBLICATION OR REPORT NUMBER
NISTIR 4569

2. PERFORMING ORGANIZATION REPORT NUMBER

3. PUBLICATION DATE
APRIL 1991

4. TITLE AND SUBTITLE
Analysis of Optical Flow Estimation using Epipolar Plane Images.

5. AUTHOR(S)
Ramesh Rangachar, Tsai-Hong Hong, Martin Herman and Randall Luck

6. PERFORMING ORGANIZATION (IF JOINT OR OTHER THAN NIST, SEE INSTRUCTIONS)
U.S. DEPARTMENT OF COMMERCE
NATIONAL INSTITUTE OF STANDARDS AND TECHNOLOGY
GAITHERSBURG, MD 20899

7. CONTRACT/GRANT NUMBER

8. TYPE OF REPORT AND PERIOD COVERED

9. SPONSORING ORGANIZATION NAME AND COMPLETE ADDRESS (STREET, CITY, STATE, ZIP)

10. SUPPLEMENTARY NOTES

11. ABSTRACT (A 200-WORD OR LESS FACTUAL SUMMARY OF MOST SIGNIFICANT INFORMATION. IF DOCUMENT INCLUDES A SIGNIFICANT BIBLIOGRAPHY OR LITERATURE SURVEY, MENTION IT HERE.)

Image flow, the apparent motion of brightness patterns on the image plane, can provide important visual information such as distance, shape, surface orientation, and boundaries. It can be determined by either feature tracking or spatio-temporal analysis. We consider spatio-temporal methods, and show how differential range can be estimated from time-space imagery.

We generate a time-space image by considering only one scan line of the image obtained from a camera moving in the horizontal direction at each time interval. At the next instant of time, we shift the previous line up by one pixel, and obtain another line from the image. We continue the procedure to obtain a time-space image, where each horizontal line represents the spatial relationship of the pixels, and each vertical line the temporal relationship.

Each feature along the horizontal scan line generates an edge in the time-space image, the slope of which depends upon the distance of the feature from the camera. We apply two mutually perpendicular edge operators to the time-space image, and determine the slope of each edge. We show that this corresponds to optical flow. We use the result to obtain the differential range, and show how this can be implemented on the Pipelined Image Processing Engine (PIPE).

We use a simple technique to calibrate the camera and show how the depth can be obtained from optical flow. We provide a statistical analysis of the results of 3-D reconstruction of the scenes using optical flow determined from 3x3, 5x5, and 7x7 edge operators.

12. KEY WORDS (6 TO 12 ENTRIES; ALPHABETICAL ORDER; CAPITALIZE ONLY PROPER NAMES; AND SEPARATE KEY WORDS BY SEMICOLONS)
Differential Range, Edge operators, EPI, Feature Tracking, Gradient Based Methods, Misclassified points, Optical Flow, PIPE, Spatio-temporal image, Zero crossings

13. AVAILABILITY

X	UNLIMITED
	FOR OFFICIAL DISTRIBUTION. DO NOT RELEASE TO NATIONAL TECHNICAL INFORMATION SERVICE (NTIS).
	ORDER FROM SUPERINTENDENT OF DOCUMENTS, U.S. GOVERNMENT PRINTING OFFICE, WASHINGTON, DC 20402.
X	ORDER FROM NATIONAL TECHNICAL INFORMATION SERVICE (NTIS), SPRINGFIELD, VA 22161.

14. NUMBER OF PRINTED PAGES
13

15. PRICE
A02

ELECTRONIC FORM